

## The binding of polyvalent galactosides to the lectin *Ricinus communis* agglutinin 120 (RCA<sub>120</sub>): an ITC and SPR study†

Sebastian G. Spain<sup>\*a</sup> and Neil R. Cameron<sup>\*b</sup>

Received 19th January 2011, Accepted 10th March 2011

DOI: 10.1039/c1py00030f

Mono- and polyvalent galactosides have been investigated with respect to their binding to the plant lectin *Ricinus communis* agglutinin 120 (RCA<sub>120</sub>). Thermodynamic parameters ( $K_a$ ,  $\Delta G$ ,  $\Delta H$ ,  $\Delta S$  and  $n$ ) have been determined by isothermal titration calorimetry (ITC) and kinetics of binding ( $k_a$  and  $k_d$ ) measured by surface plasmon resonance (SPR). ITC analysis using a single set of sites model found a non-statistical increase in avidity with increasing valency with the largest ligand displaying a greater than 20-fold increase in  $K_a$  compared to its monomeric precursor after correction for valency; binding was found to be enthalpically driven. SPR analysis supports the avidity increase but values of  $K_a$  observed were up to 100-fold greater than those measured by ITC. The large discrepancy between the two measurements is rationalized by the polyvalent–polyvalent interaction that is measured by SPR.

### 1 Introduction

Many biological recognition events are mediated *via* binding interactions between carbohydrates and carbohydrate-binding proteins known as lectins. The interaction between carbohydrates and lectins is unusually weak compared to others in Nature with association constants typically in the millimolar range (*cf.*  $10^5$ – $10^{10}$  M<sup>-1</sup> for enzyme–substrate or antibody–antigen interactions). Despite this weakness of binding carbohydrate–lectin interactions display high specificity; it is uncommon to find a lectin that binds both galactose and glucose, although some variation in structure is allowed.<sup>1</sup> The ubiquity and specificity of lectins makes them an attractive targeting mechanism for drug-delivery, an area that has recently been reviewed,<sup>2</sup> but for this to be successful an increase in avidity is required. Here, as is often the case, Nature has already provided a solution – multivalency – lectins and their corresponding ligands are usually presented in clustered arrays of high valency. The increased avidity through multivalency is unusual as the relationship is non-linear and thus not an artifact of increased local concentration. This was well illustrated by Lee *et al.* who found that lectin-binding of lactosamine derivatives increased over 100-fold when the number of carbohydrate moieties was

increased from 1 to 4<sup>3</sup> and have dubbed this the *cluster glycoside effect*.<sup>4,5</sup> In the decades since Lee *et al.*'s discovery there has been much research into the cluster glycoside effect and its origins.<sup>5</sup> Several mechanisms for the enhanced avidity have been postulated including the chelate effect, where a ligand binds to multiple sites on the same lectin simultaneously,<sup>6</sup> and “bind and slide”, where lectins can diffuse internally between carbohydrates on the same ligand.<sup>7</sup>

To further investigate the cluster glycoside effect, access to multivalent ligands is required. Multivalent glycoconjugates based upon dendrimers, lipids (*e.g.* micelles and liposomes) and nanoparticles have been investigated with regard to their lectin binding but are often, in the case of dendrimers, difficult to synthesise or, for lipids and nanoparticles, their structures are ill-defined making elucidation of structure–activity relationships, and subsequent mechanistic derivation, complex. Glycopolymers are a family of glycoconjugates based upon synthetic polymer backbones that are of interest as drug-delivery vehicles and macromolecular therapeutics due to their ability to access the cluster glycoside effect using relatively facile chemistry.<sup>8</sup> Recent developments in polymer chemistry have allowed the synthesis of complex, polyvalent glycopolymers of defined valency and architecture;<sup>9,10</sup> consequently they have been studied extensively with respect to lectin binding.<sup>11</sup>

Herein we describe the synthesis of a series of mono- and polyvalent galactoside ligands *via* reversible addition–fragmentation chain transfer (RAFT) polymerisation; their interactions with the plant lectin *Ricinus communis* agglutinin 120 by isothermal titration calorimetry and surface plasmon resonance and the implications of these with respect to the origins of the cluster glycoside effect.

<sup>a</sup>School of Pharmacy, Boots Science Building, University of Nottingham, Nottingham, NG7 2RD, UK. E-mail: sebastian.spain@nottingham.ac.uk; Tel: +0115 8466241

<sup>b</sup>Department of Chemistry, University of Durham, University Science Laboratories, South Road, Durham, DH1 3LE, UK. E-mail: n.r.cameron@durham.ac.uk; Tel: +0191 3342008

† Electronic Supplementary Information (ESI) available: Solution size distributions of polymeric ligands by dynamic light-scattering. See DOI: 10.1039/c1py00030f

## 2 Results and discussion

### 2.1 Synthesis of galactoside ligands

2-( $\beta$ -D-galactosyloxy)ethyl methacrylate (**1**) was synthesised in two steps from  $\beta$ -D-galactose pentaacetate and 2-hydroxyethyl methacrylate (HEMA) *via* boron trifluoride promoted glycosylation (Fig. 1).<sup>12,13</sup> Glycosyl 2-*O*-acetates are considered to be “disarmed”, that is they are relatively poor glycosyl donors, and consequently require long reaction times to achieve high levels of glycosylation. Deng *et al.* recently reported the acceleration of Lewis acid promoted glycosylation by the use of sonication<sup>14</sup> and, when used in conjunction with an excess of the glycosyl donor, complete glycosylation of HEMA was achieved in 45 min with no loss of anomeric selectivity. After deprotection and purification by standard methods the desired product was isolated in good yield (typically  $\sim$ 50% overall).

Polyvalent ligands were synthesised by RAFT polymerisation of **1** in aqueous ethanol using (4-cyanopentanoic acid)-4-dithiobenzoate and 4,4'-azobis(4-cyanopentanoic acid) as the chain transfer agent (CTA) and initiator respectively; different valencies were targeted by varying the [monomer]/[CTA] ratio. Residual **1** and other low molecular weight impurities were removed by thorough dialysis against high purity water (MWCO 3.5 kDa). Molecular weights, polydispersity indices and hydrodynamic radii were determined using aqueous size exclusion chromatography and dynamic light-scattering; the average valency of each ligand was determined from the value of  $M_n$  (Table 1).

### 2.2 Binding interactions between RCA<sub>120</sub> and galactoside ligands

The binding between the lectin *Ricinus communis* agglutinin 120 (RCA<sub>120</sub>) and a series of  $\beta$ -D-galactose bearing ligands was subjected to two forms of analysis: isothermal titration calorimetry (ITC) and surface plasmon resonance (SPR). Although these techniques provide similar information regarding binding events they are complementary, allowing investigation of different aspects of the binding event. ITC allows the determination of the thermodynamics of a binding event and can thus provide an insight into its mechanism, for example entropically driven events are likely to involve the displacement of water or other small ligands from the protein binding site.<sup>15</sup> SPR is more comparable to how the binding event may occur *in vivo*, where it is likely that lectins will be clustered on a cell surface with the ligand flowing past transiently. RCA<sub>120</sub> was chosen because initial SPR studies using peanut agglutinin (PNA) found the

binding to be so weak as to be undetectable by this method. This is unlikely to be due to genuinely weak interaction with the polymers as their binding to PNA has previously been demonstrated by ITC.<sup>16</sup> Instead, it is likely to be due to the lectin binding preferentially to the carboxylated methylcellulose coating on the SPR chip to which it is attached covalently preventing the ligand access to its recognition domain. Similar effects have been reported before by Kamerling *et al.*<sup>17</sup>

### 2.3 Isothermal titration calorimetry

Isothermal titration calorimetry has previously been used to investigate the binding of poly[2-( $\beta$ -D-galactosyloxy)ethyl methacrylate] to PNA. The polymers investigated were synthesised by standard free radical polymerisation, consequently molecular weight was uncontrolled and those investigated were disparate: one low ( $M_n \sim$  3 kDa,  $M_w/M_n = 2.15$ ), the other high ( $M_n \sim$  461 kDa,  $M_w/M_n = 2.21$ ).<sup>16</sup> Here a set of polymers of intermediate molecular weights ( $20 \leq M_n \leq 60$  kDa), in addition to the monomeric species, were compared with respect to their binding to RCA<sub>120</sub>. Experiments were conducted by a standard protocol and heats of dilution/mixing were determined by titration of the carbohydrate ligands into buffer alone and subtracted from the values for ligand–lectin binding. In all cases the Wiseman parameter,  $c$ , was in the range 1–100.<sup>18</sup> Calorimetry data was analysed using Origin 7.0 Pro (OriginLab). Due to its potential toxicity, RCA<sub>120</sub> was not commercially available as a lyophilised powder, only as a buffered solution. Consequently RCA<sub>120</sub> was buffer exchanged prior to use to ensure the same buffers were used for both ligand and receptor. The concentration of the resulting solution was determined by UV spectroscopy using a value of  $A^{1\%}$  of 15.7 at 280 nm.<sup>19</sup> Some RCA<sub>120</sub> precipitation was observed upon storage, consequently concentrations were redetermined prior to each experiment.

The previous study on poly[2-( $\beta$ -D-galactosyloxy)ethyl methacrylate] binding to PNA noted that the “single set of sites” model (SSoS) within the ITC software did not produce adequate fitting to derive thermodynamic parameters; a problem attributed to precipitation of polymer–protein aggregates formed upon binding.<sup>16</sup> Instead they used a more complex model that introduced a second enthalpic term to allow for the heat change due to the precipitation. However, it should be noted that greatest enthalpic contribution for precipitation observed was for the monomeric ligand **1** which should be incapable of causing lectin precipitation through multiple binding and questions the validity of this model. Additionally RCA<sub>120</sub> is approximately half the size of PNA and only has 2 carbohydrate binding sites

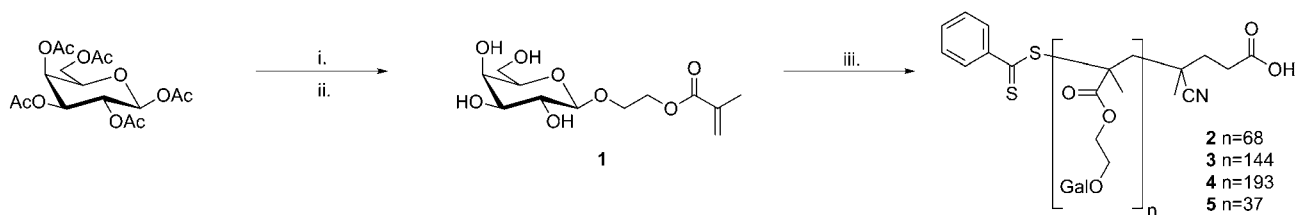


**Fig. 1** Synthesis of the mono- and polyvalent ligands studied. Reaction conditions: i. 2-hydroxyethyl methacrylate,  $\text{BF}_3 \cdot \text{Et}_2\text{O}$ , DCM, sonication; ii. damp MeOH,  $\text{K}_2\text{CO}_3$ ; iii. (4-cyanopentanoic acid)-4-dithiobenzoate, 4,4'-azo(4-cyanopentanoic acid), water/EtOH, 70 °C.

**Table 1** Molecular weight and size data for the ligands studied

Ligand	$M_n^a$ (kDa)	$M_w/M_n^a$	Valency	$D_h^b$ (nm)	$D_h^c$ (nm)	$l^d$ (nm)
1	n/a	n/a	1	n/a	n/a	
2	20.1	1.15	68	5.4	6.6	17.2
3	42.3	1.11	144	8.0	7.2	36.2
4	56.6	1.10	193	23.4	30.8	46.6
5	11.0	1.10	37	4.6	5.2	9.3

<sup>a</sup> Measured using triple detection aqueous size exclusion chromatography. <sup>b</sup> Determined by dynamic light-scattering in HEPES buffer. <sup>c</sup> Determined by dynamic light-scattering in PBS. <sup>d</sup> Approximate fully extended chain length assuming a C–C bond length of 1.54 Å and a dihedral angle of 109.5°.

(*cf.* 4 on PNA) making lectin cross-linking less likely and Brewer *et al.* have reported successful derivation of thermodynamic parameters with multivalent ligands using the SSoS model when the concentrations of ligand and lectin were such that no precipitation was observed.<sup>20, 21</sup> Here, although a small quantity of precipitation was observed when the largest ligand was used, the SSoS model was found to fit adequately. Fig. 2 contains example raw calorimetry data, binding isotherm and curve of best fit for the binding between ligand 3 and RCA<sub>120</sub>. Despite the relatively poor quality of the raw data (Fig. 2A), baseline correction and processing within the software resulted in an isotherm with the expected sigmoidal shape and fitting resulted in a curve in close agreement to the data. As the RCA<sub>120</sub> tetramer is known to have two identical binding sites<sup>19</sup>  $n$  was fixed at 2 for monomeric species to simplify fitting. The ITC data were also analysed using a modified Scatchard analysis previously described by Brewer *et al.*<sup>20,21</sup> This methodology introduces an additional term for the functional valency of the ligand allowing the construction of Scatchard plots for multivalent ligands (see Materials and methods for details).

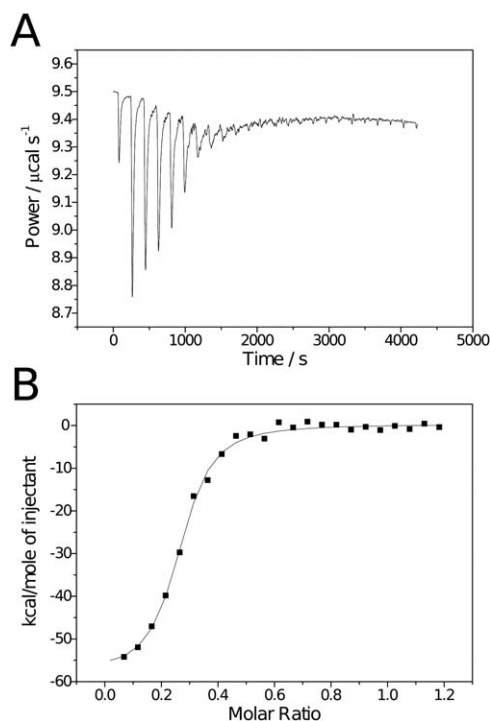


**Fig. 2** Raw (A) and processed (B) isotherms for the binding of polymeric ligand 3 to RCA<sub>120</sub>.

**2.3.1 Thermodynamic basis of binding.** Fig. 3A and Table 2 contain the thermodynamic parameters determined from ITC data using the SSoS model. For all ligands tested the binding is enthalpically driven with enthalpy–entropy compensation. For

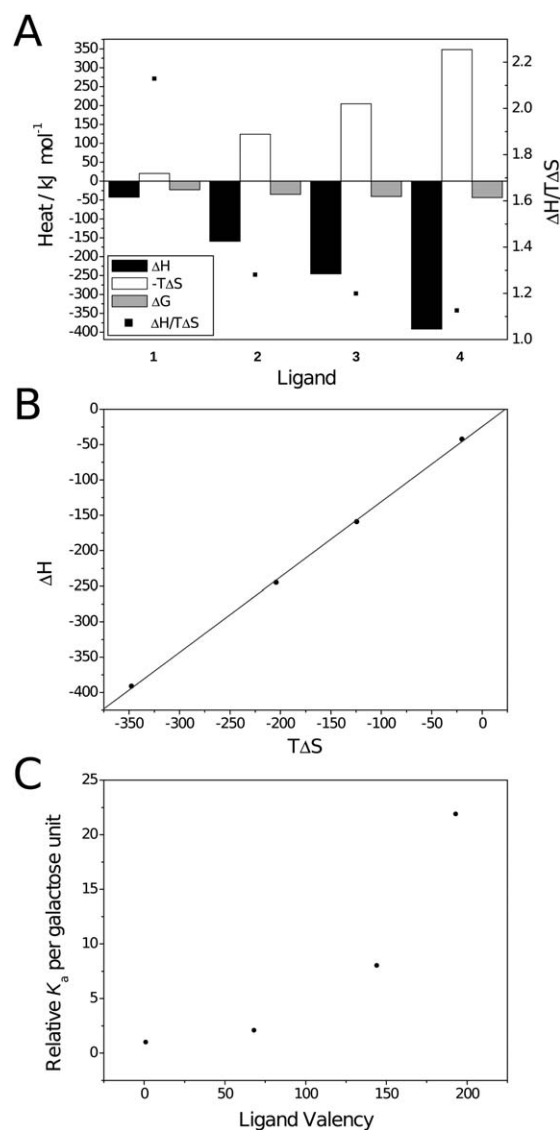


**Fig. 3** Thermodynamic plots for the binding between galactoside ligands and RCA<sub>120</sub>. (A) Thermodynamic parameters; (B) Compensation plot (—) Linear fit.  $R^2 = 0.999$ , slope = 1.06; (C) Valency corrected  $K_a$  versus ligand valency.

**Table 2** Thermodynamic parameters for the binding between RCA<sub>120</sub> and galactoside ligands as determined by isothermal titration calorimetry using a single set of sites model

Ligand	$\Delta H_{\text{obs}}^a$ (kJ mol <sup>-1</sup> )	$\Delta G_{\text{obs}}^a$ (kJ mol <sup>-1</sup> )	$T\Delta S_{\text{obs}}^a$ (kJ mol <sup>-1</sup> )	$K_a/\text{M}^{-1}$		$\beta^c$	$n^d$	$1/n$
				SSoS <sup>b</sup>	Scatchard			
1	-42.4	-22.5	-19.9	$8.74 \times 10^3$	$7.19 \times 10^3$	1	2 <sup>e</sup>	0.5
2	-159	-34.8	-124	$1.24 \times 10^6$	$1.06 \times 10^6$	140	0.224	4.46
3	-245	-40.7	-204	$1.01 \times 10^7$	$9.87 \times 10^6$	1155	0.255	3.92
4	-391	-43.7	-347	$3.69 \times 10^7$	$3.58 \times 10^7$	4222	0.130	7.69
3 <sup>f</sup>	-242	-40.1	-202	$1.07 \times 10^7$	n/a	1224	0.260	3.85

<sup>a</sup> As molarities rather than activities were used the values are reported as observed. <sup>b</sup> "Single set of sites" model. <sup>c</sup> Defined as the ratio of polyvalent and monovalent interaction.<sup>22</sup> <sup>d</sup> Stoichiometry with respect to lectin, *i.e.* number of ligands per RCA<sub>120</sub> tetramer. <sup>e</sup>  $n$  was fixed during curve fitting to allow calculation of  $K$  and  $\Delta H$ . <sup>f</sup> Calculated from isotherm without subtraction of heats of dilution.

ligand **1** this has been observed previously for its binding to PNA and the enthalpic and entropic contributions are similar to those reported by Ambrosi *et al.*<sup>16</sup> For methyl- $\beta$ -D-galactoside binding to RCA<sub>120</sub><sup>19</sup> the same enthalpy-entropy compensation is observed but the enthalpic gain and entropic loss are higher in this case. This is likely to arise from the additional hydrogen bonds and Van der Waals forces between the ethylmethacrylate section of **1** and RCA<sub>120</sub> that increase the enthalpic contribution but with a reduction in degrees of freedom and a larger entropic loss. The result is an overall avidity ( $K_a$   $8.74 \times 10^3$  M<sup>-1</sup>) similar to those reported by Ambrosi *et al.* ( $K_a$   $5.65 \times 10^3$  M<sup>-1</sup> for **1** to PNA<sup>16</sup>) and Sharma *et al.* ( $K_a$   $7.7 \times 10^3$  M<sup>-1</sup> for methyl- $\beta$ -D-galactoside to RCA<sub>120</sub> at 15 °C).<sup>19</sup>

For the polyvalent ligands, enthalpically driven binding is contrary to both modelled behaviour for multivalent binding<sup>23</sup> and that reported by Ambrosi *et al.*<sup>16</sup> The enthalpic driving force is confirmed by the compensation plot (Fig. 3B) which is linear with a slope greater than unity ( $1.06 \pm 0.02$ ;  $R^2 = 0.999$ ). The difference in thermodynamic behaviour between the two lectin bindings is probably due to a combination of effects. Ambrosi *et al.* partly attributed the entropic factor to displacement of water from the protein surface through aggregation. As aggregation was only observed to a slight degree here less of an entropic factor is likely. Similar behaviour has been reported by Brewer *et al.* for lectin binding of dendritic multivalent carbohydrates when aggregation was absent.<sup>20,21,24</sup> Ambrosi *et al.* also noted that thermodynamic parameters were heavily influenced by ionic strength of the buffer used in the titration. Higher concentrations of salts resulted in an increased enthalpic contribution and a reduced entropic contribution;  $K_a$  was also reduced dramatically. This was particularly prominent when tris buffer was used, instead of citrate, with the binding becoming entropically disfavoured. It should also be noted that, due to the high heat of ionisation of tris ( $\Delta H_{\text{ion}} \sim 46$  kJ mol<sup>-1</sup>),<sup>25</sup> values may not have been completely accurate. Here, phosphate-buffered saline was used for all experiments due to the high solubility of RCA<sub>120</sub> in this solution and its heats of ionisation being relatively low ( $-1 \leq \Delta H_{\text{ion}} \leq 4$  kJ mol<sup>-1</sup> depending on ionic strength).<sup>25</sup> The minimal effect of buffer ionisation is confirmed by comparison of the thermodynamic parameters calculated with and without correction for heats of dilution/mixing for ligand **3** (entries 3 and 5 in Table 2) confirming that the lack of entropic contribution is not due to buffer choice.

Entropic favourability would also be likely if lectin binding leads to dispersion of polymer aggregates. Glycopolymers have already been shown to self-associate in aqueous solution<sup>26</sup> with association attributed to intermolecular hydrogen bonding and hydrophobic interactions by the polymer backbone. Dynamic light-scattering at the same concentration used for ITC (see Table 1 for hydrodynamic diameters and ESI† for distributions) showed no evidence of aggregation for ligands **2** and **3**. Ligand **4** is larger than expected when compared to the other ligands having a hydrodynamic radius 4-fold greater than ligand **3** despite only a <50% increase in molecular weight. It is unclear if this is due to aggregation as there is no evidence of a smaller species consistent with the unimolecular, unaggregated polymer and analysis at a 10-fold lower concentration showed no change in hydrodynamic radius. Consequently the large difference in hydrodynamic radius for ligands **3** and **4** may instead be due to a change in solution conformation with increasing molecular weight. Although dispersion of possible aggregates during binding is still a possibility the apparent solution stability of **4** suggests that these effects may be negligible. Overall binding would be expected to be entropically disfavoured as a bound polymer will have fewer possible solution conformations and thus a reduced number of degrees of freedom. This is particularly true where ligands are binding to multiple lectin moieties which both restricts the degrees of freedom and reduces the number of discrete species in solution.

Interestingly, as molecular weight increases, the ratio  $\Delta H/T\Delta S$  decreases and tends towards 1 (black squares in Fig. 3A). Similar behaviour has been noted in dendritic systems where  $\Delta H$  was seen to scale approximately with valency, *i.e.* for a tetravalent system  $\Delta H$  was approximately 4-fold that of the monovalent, but  $-T\Delta S$  became more positive disproportionately.<sup>27</sup> This behaviour was attributed to the inability of a relatively rigid ligand to fill both binding sites on an individual lectin, instead binding one lectin for each ligand presented, resulting in a greater entropic cost. The same explanation is possible here as, although the ligands in question are relatively flexible molecules, the two binding sites on RCA<sub>120</sub> are approximately 11 nm apart (measured with Jmol<sup>28,29</sup> using the Protein Data Bank file 1RZO<sup>30</sup>). The hydrodynamic diameter and fully extended chain lengths of ligands **2-4** are given in Table 1. From these it may be possible for **3** and **4** to bridge both sites but to do so would come at great entropic cost due to the restriction of the degrees of

freedom on the polymer's conformation; particularly ligand **3** which would be very extended. Consequently it may be more entropically favourable to bind a single site of multiple RCA<sub>120</sub> molecules which is supported by the values of  $1/n$  (the number of lectins per ligand). Unsurprisingly the stoichiometry of the interaction also varies considerably with valency. More interestingly there is a decrease in stoichiometry between ligands **2** and **3**. This may be an artifact of imperfect fitting of the SSoS model and will be discussed in more detail (*vide infra*).

**2.3.2 Dependence of avidity on valency.** Values of  $K_a$  determined by the SSoS model and a modified Scatchard analysis described by Brewer *et al.*<sup>20</sup> are given in Table 2. The values of  $K_a$  from the Scatchard analysis are in good agreement with those derived by SSoS confirming its applicability under these conditions. From these data it is clear that binding avidity to RCA<sub>120</sub> is greatly enhanced through multivalency with  $K_a$  rising rapidly with increasing valency (Fig. 3C).

Ligand **4** (average valency 193) has an overall avidity over 4000-fold greater than monomeric ligand **1**; on a per sugar basis this 22-fold increase is no less striking. The non-linear behaviour observed is similar to that demonstrated by Kiessling *et al.* who also found a limiting molecular weight after which avidity no longer increased; this may also be the case here but would require larger ligands to be synthesised and analysed.<sup>6,31</sup> Kiessling *et al.* attributed the large increase to the larger ligands' ability to bridge binding sites on a single lectin.

#### 2.4 SPR analysis of multivalent–multivalent interactions between polyvalent galactoside ligands and RCA<sub>120</sub>

Several reports of studies of the interaction of glycopolymers with lectins *via* SPR have been published.<sup>31–35</sup> Only one has studied the interaction between an immobilised lectin and a glycopolymer in solution,<sup>35</sup> the configuration closest to that likely *in vitro* and *in vivo*, and the one that allows investigation of the multivalent–multivalent interaction that occurs at a cell surface prior to *e.g.* endocytosis. For the experiments RCA<sub>120</sub> was attached to the surface of a sensor chip at various levels of functionalisation (*ca.* 200, 2000 and 5000 response units) using a standard amine coupling protocol. Solutions of ligands **3** and **5**, ranging in concentration from 500 pM to 10 μM, were prepared and analysed for the binding to each channel. Initial test runs found the binding to be too tight, with very long off times. To reduce this time, allowing rapid acquisition of another sample, an injection of methyl β-D-galactoside solution was performed. The blank was subtracted from the functionalised channels to allow for non-specific binding. The channels with the lowest and highest levels of RCA<sub>120</sub> modification were found to give too weak or too strong binding respectively. Sensorgrams were thus acquired on channel 2 (*ca.* 2000 RU RCA<sub>120</sub>) by a 180 s injection of the ligand and a 240 s off period. Between acquisitions a 30 s injection of methyl β-D-galactoside and 60 s off period were performed to return the surface to its background level.

Sensorgrams for the two ligands at various concentrations are shown in Fig. 4. The data from these were fitted within the BIAcore software using a single sites (1 : 1 Langmuir Binding) model. For each polymer five consecutive concentrations were chosen from those analysed; 5 nM–1 μM for ligand **5** and 500

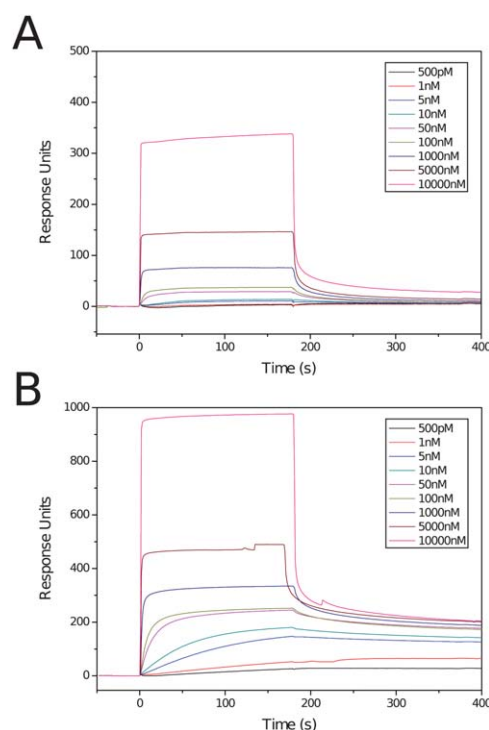


**Fig. 4** SPR sensorgrams for the binding of ligand **5** (A) and **3** (B) to RCA<sub>120</sub>-modified sensor chip.

pM–50 nM for ligand **3**. The highest concentrations were removed as the binding was too rapid to enable accurate fitting. For ligand **5**, the lowest two concentrations were removed as the response was too weak to allow accurate fitting. Thermodynamic and kinetic parameters for these polymers are shown in Table 3. As was seen with the ITC experiment, there is a large increase in  $K_a$  with increased molecular weight, here a ~4-fold increase in valency leads to a near 8-fold increase in avidity. The larger polymer also displays more than a 100-fold increase in  $K_a$  compared to the value measured by ITC ( $1.39 \times 10^9 \text{ M}^{-1}$  *cf.*  $1.01 \times 10^7 \text{ M}^{-1}$ ); an increase attributable to the now multivalent–multivalent interaction. The kinetic parameters for the two ligands are more interesting. Despite the large difference in  $K_a$  there is less than a 2-fold difference in the association rate constant,  $k_a$ . Looking at this value alone it would be expected that these ligands would have similar avidities. However, ligand **5** has a value of  $k_d$  5-fold higher than that of ligand **3** and, consequently, has a far lower avidity ( $K_a = k_a/k_d$ ).

**Table 3** Kinetic and thermodynamic parameters of binding between RCA<sub>120</sub> and polyvalent galactoside ligands as calculated by surface plasmon resonance

Ligand	$k_a$ (1/Ms)	$k_d$ (1/s)	$K_a$ (M <sup>-1</sup> )	$\Delta G_{\text{obs}}^a$ (kJ mol <sup>-1</sup> )
5	$9.54 \times 10^5$	$5.28 \times 10^{-3}$	$1.81 \times 10^8$	-47.1
3	$1.56 \times 10^6$	$1.12 \times 10^{-3}$	$1.39 \times 10^9$	-52.2
Ratio (3/5)	1.6	0.2	7.7	

<sup>a</sup> Calculated from  $K_a$ .

## 2.5 Origins of the cluster glycoside effect in polyvalent galactosides

The thermodynamic and kinetic data above provide evidence that the avidity enhancement between polyvalent galactosides and RCA<sub>120</sub> compared to their monomeric analogues has contributions from both the chelation mechanism used by Kiessling *et al.*<sup>6,31</sup> and the “bind and slide/hop” mechanism observed with multivalent carbohydrates and mucins by Brewer *et al.*<sup>7,20,21,36</sup> As observed by Kiessling *et al.* there is an exponential increase in avidity with valency. The small solution size of ligands **2** and **3** make it unlikely that they can bind both sites of RCA<sub>120</sub> at least without considerable entropic cost, suggesting that the avidity increase is due to a “bind and slide” mechanism similar to that described by Brewer *et al.* A suggested mechanism of binding is proposed in Fig. 5. For the early injections, where the concentration of RCA<sub>120</sub> is far greater than that of the ligand, ligands are rapidly bound by the excess lectin and a core-shell structure is formed with the ligand at the centre; as the shell is composed of lectin alone cross-linking is unable to occur. As the ligand concentration is increased a second shell of ligand is formed around the first creating a glycosylated shell that, again, prevents cross-linking and macroscopic precipitation. The far smaller size of the ligand compared to the ligand-lectin aggregates and, consequently, their higher diffusion rate makes formation of the multi-layer structure kinetically favourable compared to the formation of crosslinks. The reduced mobility of RCA<sub>120</sub> and the ligands results in a dynamic equilibrium where an unbinding event is rapidly counteracted by rebinding of a galactose moiety on the same or a neighbouring ligand. This mechanism is supported by the enthalpic nature of the interaction and disfavoured entropic factor. Investigation of the solution structure throughout the binding experiment may allow elucidation of this mechanism. For ligand **4**, which appears to have a larger, possibly extended, structure in solution, it is likely that the same mechanism is occurring but, due to its lower mobility, it is kinetically less favoured for multi-layer structures to form before macroscopic precipitation can occur.

The SPR data also supports a “bind and slide” type mechanism. Ligand **5** is too small to be able to bind both sites on RCA<sub>120</sub> as its fully extended chain length is  $\leq 10$  nm. It is also unlikely that it could bind two neighbouring lectins on the surface as the modification density was relatively low. Consequently its high avidity for the lectin-coated surface can only

arise from rapid association following a dissociation event resulting in a low overall dissociation rate. **3** may be able to bind two sites simultaneously but to do so would require a conformational change compared to its solution structure and the SPR “two state-conformational change” model was found to fit poorly to the data. Additionally, the increased avidity of **3** *cf.* **5** is dominated by a decreased off rate which is in agreement with a “bind and slide” type mechanism and an increased probability of rebinding. If the ligands are approximated to a deformable sphere then they can be considered to have a footprint that will be proportional to their radius. In the same manner, a tyre of a larger diameter will maintain a larger contact area with the road than a smaller one; assuming all other factors to be the same. Deformable spheres have been modelled to roll along ‘sticky’, *i.e.* interacting, surfaces,<sup>37,38</sup> a phenomenon that has also been modelled and observed experimentally in leukocytes.<sup>39,40</sup> An increased contact area during rolling will result in a greater probability of secondary binding events occurring, resulting in increased retention on the surface. Thus smaller polymers, with their reduced footprints will be shed more readily, increasing  $k_d$  values.

## 3 Materials and methods

### 3.1 Materials

(4-Cyanopentanoic acid)-4-dithiobenzoate was synthesised according to literature<sup>41</sup> and isolated as a pink crystalline solid.  $\beta$ -D-Galactose pentaacetate (98%), 2-hydroxyethyl methacrylate (98%, HEMA) and potassium carbonate (99%) were purchased from Aldrich. Boron trifluoride diethyl etherate (*purum*, dist.) and 4,4'-azobis(4-cyanopentanoic acid) (98%) were purchased from Fluka. Amberjet 1200H strong acid cation exchange resin was purchased from Fisher. RCA<sub>120</sub> was purchased from Vector Labs and was supplied as 5 mg mL<sup>-1</sup> solution in PBS. All solvents were Fisher HPLC grade, when anhydrous solvents were required they were dried using an Innovative Technologies Pure Solv system using alumina columns and stored under nitrogen prior to use. Ultra-high quality (UHQ) water ( $\geq 18$  M $\Omega$  resistivity) was obtained using a Purite Neptune water purification system. All other chemicals were used without further purification. Gradient flash column chromatography was performed using a Biotage SP1 automated purification system using pre-packed silica columns.

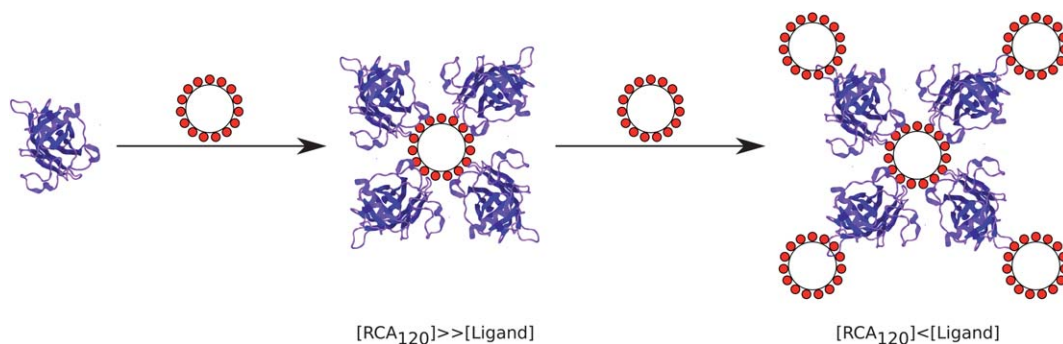


Fig. 5 Schematic of the possible binding mechanism between RCA<sub>120</sub> and polyvalent galactosides.

## 3.2 Ligand synthesis

2-( $\beta$ -D-galactosyloxy)ethyl methacrylate and its polymers were synthesised as previously described.<sup>12,13</sup>

**3.2.1 Synthesis of 2-(2',3',4',6'-tetra-O-acetyl- $\beta$ -D-galactosyloxy)ethyl methacrylate.**  $\beta$ -D-Galactose pentaacetate (5.0 g, 12.8 mmol) and 2-hydroxyethyl methacrylate (1.4 mL, 1.5 g, 11.5 mmol) were dissolved in anhydrous dichloromethane (20 mL) and sonicated under a blanket of anhydrous N<sub>2</sub> for 5 min; subsequently, BF<sub>3</sub>·Et<sub>2</sub>O (5.0 mL, 5.75 g, 40.5 mmol) was added *via* syringe and the solution was sonicated for a further 45 min. The reaction mixture was washed with brine (30 mL), the organic layer dried over MgSO<sub>4</sub> and butylhydroxytoluene was added as an inhibitor. The solvent was removed under reduced pressure, yielding crude the product as a yellow oil which was used directly for the synthesis of 2-( $\beta$ -D-galactosyloxy)ethyl methacrylate. A sample for analysis was purified by flash column chromatography (7 : 3, hexane–ethyl acetate).

Found C, 51.88; H, 6.18; C<sub>20</sub>H<sub>28</sub>O<sub>12</sub> requires C, 52.17; H, 6.13. FT-IR  $\nu$ /cm<sup>-1</sup>: 1751 (C=O of acetate groups) 1719 (C=O of methacrylate ester) 1637, 1320, 1298 (C=C).  $\delta_{\text{H}}$ : (400 MHz, CDCl<sub>3</sub>) 1.98 (3H, s, 3 × H-3), 2.01, 2.04, 2.05, 2.15, (3H × 4, 4s, Ac × 4), 3.84 (1H, ddd,  $J_{6a, 6b}$  11.5 Hz,  $J_{5a, 6a}$  7.5 Hz,  $J_{5b, 6a}$  4.0 Hz, H-6a), 3.92 (1H, td,  $J_t = J_{5', 6a'} = J_{5', 6b'}$  6.6 Hz,  $J_d = J_{4', 5'}$  1.1 Hz, H-5'), 4.06 (1H, ddd,  $J_{6a, 6b}$  11.6 Hz,  $J_{5b, 6b}$  5.9 Hz,  $J_{5a, 6b}$  3.7 Hz, H-6b), 4.10 (1H, dd,  $J_{6'a, 6'b}$  10.3 Hz,  $J_{5', 6'a}$  6.7 Hz, H-6'a), 4.18 (1H, dd,  $J_{6'a, 6'b}$  10.9 Hz,  $J_{5', 6'b}$  6.5 Hz, H-6'b), 4.29 (2H, m, H-5a,b), 4.55 (1H, d,  $J_{1', 2'}$  8.05 Hz, H-1'), 5.01 (1H, dd,  $J_{2', 3'}$  10.4 Hz,  $J_{3', 4'}$  3.6 Hz, H-3'), 5.23 (1H, dd,  $J_{2', 3'}$  10.4 Hz,  $J_{1', 2'}$  8.0 Hz, H-2'), 5.39 (1H, dd,  $J_{3', 4'}$  4.5 Hz,  $J_{4', 5'}$  1.2 Hz H-4'), 5.59–5.61 (1H, m, H-1 Z to Me–C=C), 6.13–6.14 (1H, m, H-1 E to Me–C=C).  $\delta_{\text{C}}$ : (100.26 MHz, decoupled, <sup>1</sup>H 400 MHz; CDCl<sub>3</sub>) 18.25 (C-3), 20.6, 20.8, 21.0 (4 × H<sub>3</sub>CCO<sub>2</sub>, 2 resonances overlap), 61.3 (C-6'), 63.5 (C-5), 66.8 (C-4'), 67.4 (C-6), 68.7 (C-2'), 70.7 (C-3'), 70.9 (C-5'), 101.3 (C-1'), 125.9 (C-1), 136.1 (C-2), 167.1 (C-4), 169.4, 170.2, 170.3 (MeCO<sub>2</sub>). LR-MS (ES<sup>+</sup>)  $m/z$  requires 483.4, found 483.2 (M + Na<sup>+</sup>).

**3.2.2 Synthesis of 2-( $\beta$ -D-galactosyloxy)ethyl methacrylate.** Crude 2-(2',3',4',6'-tetra-O-acetyl- $\beta$ -D-galactosyloxy)ethyl methacrylate (2.5 g, 5.5 mmol) was stirred in damp MeOH (20 mL). K<sub>2</sub>CO<sub>3</sub> (1.0 g, 7.2 mmol) was added and the reaction was monitored by TLC (9 : 1, MeCN–H<sub>2</sub>O). When the product of methacrylate ester cleavage was seen in the TLC ( $R_f$  0.15) the reaction was neutralized by filtering into a flask containing Amberjet 1200H (H<sup>+</sup>) cation exchange resin and the mixture was stirred for 15 min. [NB: The deprotection reaction can proceed very rapidly; to prevent loss of the product due to methacrylate cleavage, ensure that the apparatus for filtration and neutralization are set up and ready for use before addition of K<sub>2</sub>CO<sub>3</sub>]. The resin was removed by filtration and the solvent was removed under reduced pressure. The resulting oil was purified by column chromatography (CHCl<sub>3</sub>–MeOH, gradient elution) to yield a colorless oil which became a white amorphous solid upon lyophilising. The product was dissolved in D<sub>2</sub>O to give a 0.50 M solution that was stored at –18 °C.

Found C, 49.12; H, 6.94; C<sub>12</sub>H<sub>20</sub>O<sub>8</sub> requires C, 49.31; H, 6.90. FT-IR (NaCl Plates)  $\nu$ /cm<sup>-1</sup>: 3360 (br, OH), 1708 (C=O of

methacrylate ester) 1636, 1320, 1298 (C=C).  $\delta_{\text{H}}$ : (500 MHz; D<sub>2</sub>O) 1.94 (3H, m, 3 × H-3), 3.48 (1H, dd,  $J_{2', 3'}$  9.7 Hz,  $J_{3', 4'}$  3.3 Hz, H-3'), 3.53 (2H, dt,  $J_t$  5.09 Hz,  $J_d$  5.7 Hz, H-5'), 3.74 (2H, m, H-6') 3.84 (1H, m, H-4') 3.86 (1H, ddd,  $J_{6a, 6b}$  11.8,  $J_{5b, 6b}$  6.0,  $J_{5b, 6a}$  3.8 Hz, H-6a) 4.12 (1H, ddd,  $J_{6a, 6b}$  11.6,  $J_{5b, 6b}$  5.9,  $J_{5a, 6b}$  3.7 Hz, H-6b) 4.29 (1H, d, 7.5, H-1') 4.35 (2H, m, H-5) 5.64 (1H, m, H-1 Z to Me–C=C) 6.14 (1H, m, H-1 E to Me–C=C);  $\delta_{\text{C}}$ : (100.62 MHz; decoupled <sup>1</sup>H 500 MHz; D<sub>2</sub>O) 18.4 (C-3), 62.5 (C-6'), 65.3 (C-5), 68.5 (C-6), 70.3 (C-4'), 72.4 (C-2'), 74.9 (C-3'), 76.7 (C-5'), 103.2 (C-1'), 126.4 (C-1), 137.7 (C-2), 168.8 (C-4). LR-MS (ES<sup>+</sup>)  $m/z$  requires 315.3, found 315.1 (M + Na<sup>+</sup>).

**3.2.3 Polymerisation of 2-( $\beta$ -D-galactosyloxy)ethyl methacrylate.** For a typical polymerisation, a GalEMA solution (1.0 mL, 0.5 M, 0.5 mmol) was introduced to a small Schlenk tube and ethanol solutions of (4-cyanopentanoic acid)-4-dithiobenzoate (175  $\mu$ L, 0.015 M, 5.0  $\mu$ mol) and 4,4'-azobis(4-cyanopentanoic acid) (83  $\mu$ L, 0.015 M, 2.5  $\mu$ mol) were added. The flask was sealed and the solution was degassed by 3 freeze-pump-thaw cycles, back-filled with N<sub>2</sub> and placed in an oil bath at 70 °C. Aliquots (100  $\mu$ L) of the polymerisation solution were removed at regular intervals under N<sub>2</sub> flow, split in two and quenched by freezing in liquid nitrogen; the pairs of samples were analysed by <sup>1</sup>H NMR and aqueous SEC to determine conversion and molecular weight respectively. The remainder of the solution was dialysed against high purity water (Pierce Snakeskin dialysis tubing; MWCO 3.5 kDa) and the purified polymer solution was lyophilized to yield a pink hygroscopic amorphous solid.

$\delta_{\text{H}}$  (500 MHz, D<sub>2</sub>O) 0.61–1.50 (3H, br, m CH<sub>3</sub>-C), 1.53–2.41 (2H, br, backbone CH<sub>2</sub>), 3.37–3.62, 3.62–3.72, 3.72–3.86, 3.86–4.02, 4.02–4.16, 4.16–4.36 (10H, protons of carbohydrate and methylene side chain), 4.44 (1H, br, anomeric proton), 7.52 (H<sub>meta, arom.</sub>), 7.70 (H<sub>para, arom.</sub>), 7.99 (H<sub>ortho, arom.</sub>). Aromatic resonances from terminal dithiobenzoate moiety.

## 3.3 Analysis

NMR spectra were recorded using a Varian Inova 500 spectrometer at 499.87 (<sup>1</sup>H) and 125.67 MHz (<sup>13</sup>C, <sup>1</sup>H decoupled at 500 MHz) or using a Bruker Avance 400 spectrometer at 400.13 MHz (<sup>1</sup>H) or 100.26 MHz (<sup>13</sup>C, <sup>1</sup>H decoupled at 400 MHz). NMR spectra were analyzed using the Varian VNMR 6.1C or MestRe Nova 5.2 software. IR spectra were recorded on a Perkin-Elmer 1600 Series FT-IR spectrometer by casting a film on NaCl plates from either DCM or MeOH. Mass spectra were acquired using a Micromass LCT spectrometer using ES<sup>+</sup> ionization. Elemental analyses were obtained using an Exeter Analytical Inc. E-440 Elemental Analyzer. Aqueous SEC was performed using a Viscotek TDA 301 SEC system fitted with two (300 × 7.5 mm) TSKgel GMPWxl columns (Tosoh Biosciences) and differential refractive index, viscometry and right-angle light-scattering detectors. The eluent was 0.2 M NaNO<sub>3</sub> and 0.1 M NaH<sub>2</sub>PO<sub>4</sub> in UHQ water at a flow rate of 1.0 mL min<sup>-1</sup> and a constant temperature of 30 °C. Calibration for detector response was achieved using a single narrow PEO standard (Polymer Labs) with  $M_p$  82,500 g mol<sup>-1</sup> and a  $dn/dc$  value of 0.133 mL g<sup>-1</sup>. A  $dn/dc$  value of 0.153 mL g<sup>-1</sup> for poly[2-( $\beta$ -D-galactosyloxy)ethyl methacrylate] was determined from the RI detector response after injection of samples of known

concentration. Values of  $M_n$ ,  $M_w/M_n$  and  $D_h$  were determined using Viscotek Omnisc 4.0 for Windows software.

### 3.4 Dynamic light-scattering

Polymeric ligands were prepared as 100  $\mu\text{M}$  solutions in either phosphate-buffered saline (10 mM phosphate buffer pH 7.8, 137 mM NaCl, 2.7 mM KCl) or HEPES-buffered saline (10 mM HEPES buffer pH 7.8, 150 mM NaCl) and allowed to equilibrate at room temperature for 16 h. Dynamic light-scattering was performed using a Viscotek 802 instrument fitted with a 50 mW 830 nm laser and detection angle of  $90^\circ$ . Laser power was adjusted to ensure a mean count rate of at least 300 kilocounts per second and 10 experiments of 3 s were recorded. Experimental correlation functions were fitted with Viscotek OMNISIZE 3.0 and hydrodynamic radii calculated *via* the Stokes–Einstein equation. Mass and number distributions were calculated using the Dextran mass model within the software.

### 3.5 Isothermal titration calorimetry

Isothermal titration calorimetry was conducted using a MicroCal VP-ITC calorimeter equilibrated at 298 K. Ligands for analysis were prepared as 100  $\mu\text{M}$  solutions in aqueous buffer (10 mM phosphate buffer pH 7.8, 137 mM NaCl, 2.7 mM KCl) and allowed to equilibrate for 24 h before degassing at 297 K. RCA<sub>120</sub> was buffer exchanged by use of centrifugal size exclusion columns (Pierce Zeba Desalting Columns) prewashed with the same buffer. After buffer exchange RCA<sub>120</sub> was further diluted in the same buffer and its concentration measured by UV absorption using an  $A^{1\%}$  value of 15.7 at 280 nm.<sup>19</sup> RCA<sub>120</sub> showed some solution instability and subsequently, prior to each experiment, the stock solution was centrifuged to remove aggregated protein and the concentration redetermined. The lectin solution was added to the sample cell ensuring no trapped air bubbles and the mixture was equilibrated to 298 K. Ligand solutions were added to RCA<sub>120</sub> as a series of injections (25 aliquots of 5  $\mu\text{L}$ ) at 3 min. intervals by means of a computer controlled syringe with constant stirring at 307 rpm. To control for ligand dilution effects the experiments were repeated in the absence of RCA<sub>120</sub> and the resulting heats subtracted during analysis. Data were analysed using Origin 7.0 Pro (OriginLab) and fitted using the “single set of sites” model incorporated into the software.

**3.5.1 Modified scatchard analysis.** Scatchard analysis was performed by the modified methodology of Brewer *et al.*<sup>20</sup> Briefly, the total concentrations of ligand ( $X_t(i)$ ) and lectin ( $M_t(i)$ ) after the  $i$ th injection and the heat evolved in that injection ( $Q(i)$ ) were extracted directly from the raw ITC file. The concentration of bound ligand is given by:

$$X_b(i) = [Q(i)/\Delta H \cdot V] + X_b(i-1) \quad (1)$$

where  $\Delta H$  is the enthalpy of binding (in  $\text{J mol}^{-1}$ ) and  $V$  is the volume of the sample cell (in mL). This allows the calculation of the concentration of free ligand after the  $i$ th injection ( $X_f(i)$ ) from:

$$X_f(i) = X_t(i) - X_b(i) \quad (2)$$

In a normal Scatchard analysis, the average number of ligands bound per lectin ( $r(i)$ ) is the ratio  $X_b(i)/M_t(i)$ . The modified Scatchard analysis introduces an additional term to allow for multivalent ligands and thus:

$$r(i) = \frac{X_b(i)[\text{average functional valency of ligand}]}{M_t(i)} \quad (3)$$

where the average functionality of ligand is the value  $1/n$  given in Table 2. Scatchard plots may then be constructed by plotting  $r(i)/X_f(i)$  versus  $r(i)$ .

### 3.6 Surface plasmon resonance

All SPR measurements were performed on a BIAcore 3000 system and RCA<sub>120</sub> was immobilised using a standard amino-coupling protocol. A CM5 sensor chip was equilibrated with HEPES buffer (10 mM HEPES pH 7.4, 150 mM NaCl, 0.005% P20 surfactant) then activated by flowing a 1 : 1 mixture of 0.1 M *N*-hydroxysuccinimide and 0.1 M *N*-ethyl-*N'*-(dimethylamino-propyl)carbodiimide over the chip for 5 min at 25  $^\circ\text{C}$  at a flow rate of 5  $\mu\text{L min}^{-1}$ . RCA<sub>120</sub> was immobilised on channels 1, 2 and 3 *via* injection of a solution (10  $\mu\text{g mL}^{-1}$  in 10 mM acetate buffer pH 4) for 7, 3 and 1 min. respectively resulting in functionalisation of the surface at 5000, 2000 and 200 response units (RU) respectively. All channels were subsequently modified by flowing a solution of ethanolamine (1 M pH 8.5) for 10 min at 5  $\mu\text{L min}^{-1}$  to produce a blank on channel 4 and remove remaining reactive groups on channels 1–3.

Polymer solutions (500 pM–10 mM) were prepared in the same HEPES buffer. Sensorgrams for each polymer concentration were recorded with a 180 s injection of polymer solution (on period) followed by 240 s of buffer alone (off period). After this time the chip was regenerated by a 30 s injection of methyl  $\beta$ -D-galactoside (1  $\text{mg mL}^{-1}$ ) and 60 s of buffer alone. After regeneration was complete the next sample was injected. For each polymer 5 consecutive concentrations were used for kinetic analysis using a single set of sites (1 : 1 Langmuir Binding) model in the BIAevaluation 4.1 software.

## 4 Conclusions

Although many studies on the binding of glycopolymers to lectins have been published (*vide supra*) few have studied the underlying thermodynamics and mechanism(s) of the interactions. Here we have studied the interaction between mono- and polyvalent galactosides synthesised from 2-( $\beta$ -D-galactosyloxy) ethyl methacrylate and the lectin *Ricinus communis* agglutinin 120 by both isothermal titration calorimetry and surface plasmon resonance. As expected, avidities were greatly enhanced *via* multivalency with more than 4000-fold increase in  $K_a$  for the largest (highest valency) ligand by ITC equivalent to a 22-fold increase on a per-sugar basis. The combined ITC and SPR data suggest that the cluster glycoside effect between glycopolymeric ligands and lectins is the product of both chelation and “bind and slide” mechanisms.

## References

- 1 M. Ambrosi, N. R. Cameron and B. G. Davis, *Org. Biomol. Chem.*, 2005, **3**, 1593–1608.

- 2 N. Yamazaki, S. Kojima, N. V. Bovin, S. Andre, S. Gabius and H. J. Gabius, *Adv. Drug Delivery Rev.*, 2000, **43**, 225–244.
- 3 Y. Lee, R. Townsend, M. Hardy, J. Lonngren, J. Arnarp, M. Haraldsson and H. Lonn, *J. Biol. Chem.*, 1983, **258**, 199–202.
- 4 Y. C. Lee and R. T. Lee, *Acc. Chem. Res.*, 1995, **28**, 321–327.
- 5 J. J. Lundquist and E. J. Toone, *Chem. Rev.*, 2002, **102**, 555–578.
- 6 M. Kanai, K. H. Mortell and L. L. Kiessling, *J. Am. Chem. Soc.*, 1997, **119**, 9931–9932.
- 7 T. K. Dam and C. F. Brewer, *Biochemistry*, 2008, **47**, 8470–8476.
- 8 S. G. Spain and N. R. Cameron, *Polym. Chem.*, 2011, **2**, 60–68.
- 9 V. Ladmiraal, E. Melia and D. M. Haddleton, *Eur. Polym. J.*, 2004, **40**, 431–449.
- 10 S. G. Spain, M. I. Gibson and N. R. Cameron, *J. Polym. Sci., Part A: Polym. Chem.*, 2007, **45**, 2059–2072.
- 11 S. R. S. Ting, G. Chen and M. H. Stenzel, *Polym. Chem.*, 2010, **1**, 1392–1412.
- 12 S. G. Spain, L. Albertin and N. R. Cameron, *Chem. Commun.*, 2006, 4198–4200.
- 13 N. R. Cameron, S. G. Spain, J. A. Kingham, S. Weck, L. Albertin, C. A. Barker, G. Battaglia, T. Smart and A. Blanazs, *Faraday Discuss.*, 2008, **139**, 359–368.
- 14 S. Deng, U. Gangadharmath and C.-W. Chang, *J. Org. Chem.*, 2006, **71**, 5179–5185.
- 15 J. Adam, M. Pokorná, C. Sabin, E. P. Mitchell, A. Imberty and M. Wimmerová, *BMC Struct. Biol.*, 2007, **7**, 36.
- 16 M. Ambrosi, N. R. Cameron, B. G. Davis and S. Stolnik, *Org. Biomol. Chem.*, 2005, **3**, 1476–1480.
- 17 K. M. Halkes, A. C. d. Souza, C. E. P. Maljaars, G. J. Gerwig and J. P. Kamerling, *Eur. J. Org. Chem.*, 2005, 3650–3659.
- 18 T. Wiseman, S. Williston, J. F. Brandts and L.-N. Lin, *Anal. Biochem.*, 1989, **179**, 131–137.
- 19 S. Sharma, S. Bharadwaj, A. Surolia and S. K. Podder, *Biochem. J.*, 1998, **333**, 539–542.
- 20 T. K. Dam, R. Roy, D. Pagé and C. F. Brewer, *Biochemistry*, 2002, **41**, 1351–1358.
- 21 T. K. Dam, H.-J. Gabius, S. André, H. Kaltner, M. Lensch and C. F. Brewer, *Biochemistry*, 2005, **44**, 12564–12571.
- 22 M. Mammen, S.-K. Choi and G. M. Whitesides, *Angew. Chem., Int. Ed.*, 1998, **37**, 2754–2794.
- 23 P. I. Kitov and D. R. Bundle, *J. Am. Chem. Soc.*, 2003, **125**, 16271–16284.
- 24 D. K. Mandal, N. Kishore and C. F. Brewer, *Biochemistry*, 1994, **33**, 1149–1156.
- 25 S. A. Bernhard, *J. Biol. Chem.*, 1956, **218**, 961–969.
- 26 Y.-Z. Liang, Z.-C. Li and F.-M. Li, *J. Colloid Interface Sci.*, 2000, **224**, 84–90.
- 27 T. K. Dam, R. Roy, S. K. Das, S. Oscarson and C. F. Brewer, *J. Biol. Chem.*, 2000, **275**, 14223–14230.
- 28 Jmol: an open-source Java viewer for chemical structures in 3D. <http://www.jmol.org/>.
- 29 A. Herráez, *Biochem. Mol. Biol. Educ.*, 2006, **34**, 255–261.
- 30 A. G. Gabdoulkhakov, Y. Savochkina, N. Konareva, R. Krauspenhaar, S. Stoeva, S. V. Nikonov, W. Voelter, C. Betzel and A. M. Mikhailov, PDB ID: 1RZO, 2004.
- 31 D. A. Mann, M. Kanai, D. J. Maly and L. L. Kiessling, *J. Am. Chem. Soc.*, 1998, **120**, 10575–10582.
- 32 H. Uzawa, H. Ito, P. Neri, H. Mri and Y. Nishida, *ChemBioChem*, 2007, **8**, 2117–2124.
- 33 J. Geng, G. Mantovani, L. Tao, J. Nicolas, G. Chen, R. Wallis, D. A. Mitchell, R. G. Johnson, S. D. B. Evans and D. M. Haddleton, *J. Am. Chem. Soc.*, 2007, **129**, 15156–15163.
- 34 L. Yu, M. Huang, P. G. Wnag and X. Zeng, *Anal. Chem.*, 2007, **79**, 8979–8986.
- 35 C. R. Becer, M. I. Gibson, J. Geng, R. Ilyas, R. Wallis, D. A. Mitchell and D. M. Haddleton, *J. Am. Chem. Soc.*, 2010, **132**, 15130–15132.
- 36 T. K. Dam, T. A. Herken, B. S. Cavada, K. S. Nascimento, T. R. Moura and C. F. Brewer, *J. Biol. Chem.*, 2007, **282**, 28256–28263.
- 37 A. Alexeev, R. Verberg and A. C. Balazs, *Phys. Rev. Lett.*, 2006, **96**, 148103.
- 38 A. Alexeev, R. Verberg and A. C. Balazs, *Langmuir*, 2007, **23**, 983–987.
- 39 C. Dong, J. Cao, E. J. Struble and H. H. Lipowsky, *Ann. Biomed. Eng.*, 1999, **27**, 298–312.
- 40 E. F. Krasik and D. A. Hammer, *Biophys. J.*, 2004, **87**, 2912–2930.
- 41 S. H. Thang, B. K. Chong, R. T. A. Mayadunne, G. Moad and E. Rizzardo, *Tetrahedron Lett.*, 1999, **40**, 2435–2438.